

# *In vivo* imaging of synapse formation on a growing dendritic arbor

Cristopher M Niell<sup>1,3</sup>, Martin P Meyer<sup>2,3</sup> & Stephen J Smith<sup>1,2</sup>

The form of a neuron's dendritic arbor determines the set of axons with which it may form synaptic contacts, thus establishing connectivity within neural circuits. However, the dynamic relationship between dendrite growth and synaptogenesis is not well understood. To observe both processes simultaneously, we performed long-term imaging of non-spiny dendritic arbors expressing a fluorescent postsynaptic marker protein as they arborized within the optic tectum of live zebrafish larvae. Our results indicate that almost all synapses form initially on newly extended dendritic filopodia. A fraction of these nascent synapses are maintained, which in turn stabilizes the subset of filopodia on which they form. Stabilized filopodia mature into dendritic branches, and successive iterations of this process result in growth and branching of the arbor. These findings support a 'synaptotropic model' in which synapse formation can direct dendrite arborization.

Elaboration of a dendritic arbor, and formation of appropriate synaptic connections upon that arbor, are essential to neural circuit development. However, the dynamics of these two processes, and how they are coordinated, remain to be explored. Several *in vivo* studies have described the highly dynamic process of dendritic arbor elaboration, which involves prolific extension and retraction of motile filopodia on a scale of minutes (see **Supplementary Video 1** online), as well as remodeling of branching patterns over hours<sup>1–3</sup>. Other studies have begun to elucidate genetic programs<sup>4,5</sup>, extracellular guidance cues<sup>6</sup>, effects of synaptic activity<sup>7</sup> and inter- and intra-cellular signaling pathways<sup>8,9</sup> that shape the dendritic arbor<sup>10–13</sup>. Likewise, *in vitro* studies have examined the sequence of molecular events that assemble postsynaptic structures<sup>14–18</sup>. However, many questions remain at the interface of these two areas. For example, where and how are synapses formed in relation to the growth of a dendrite? Are dendritic filopodia involved in establishing synaptic contact, growth of the arbor, or both<sup>19,20</sup>? And in particular, what causes certain dendritic extensions to be stabilized when most are retracted? It is crucial to address such issues of growth and stability *in vivo*, within the natural three-dimensional (3D) substrate, under normal physiological conditions and with intact sensory and synaptic activity. We thus developed a system for long-term two-photon time-lapse imaging over multiple days of dendrite growth and synaptogenesis in tectal neurons of living zebrafish.

## RESULTS

### PSD punctum formation and dendrite growth are concurrent

To visualize synapse formation, PSD-95 (SAP-90), a scaffolding protein known to localize to the postsynaptic density (PSD) of excitatory synapses<sup>21</sup>, was cloned from zebrafish and fused to the coding sequence of green fluorescent protein (GFP). PSD-95:GFP has been used extensively as a postsynaptic marker<sup>18,22–25</sup> and is recruited to

nascent synapses within 30 min of axodendritic contact<sup>26</sup>. A red fluorescent protein (DsRed Express) was encoded on the same plasmid as PSD-95:GFP, enabling visualization of the entire dendritic arbor, as well as allowing ratio measurements to discriminate puncta of PSD-95:GFP accumulation from volume effects.

Plasmids were injected into embryos at the 1–4 cell stage, resulting in mosaic neuronal expression, ranging from single cells to large clusters of neurons, in larval stage zebrafish. We focused our studies on type-XIV tectal neurons, which are the most numerous cell type in the tectum, have monopolar cell bodies in the deepest tectal layer, and always project apical dendrites to the most superficial retinorecipient layers. The dendrites of type-XIV neurons do not generally bear spines<sup>27</sup>.

**Figure 1a** shows expression of PSD-95:GFP in an individual tectal cell that was imaged on consecutive days from 3 days post-fertilization (d.p.f.) to 10 d.p.f. In immature tectal cells (3 d.p.f.), much of the PSD-95:GFP labeling was diffuse with some discrete puncta, but as cells matured, PSD-95:GFP became progressively more punctate in the elaborating dendritic arbor. The density and distribution of PSD-95:GFP puncta in the mature dendrite were also similar to that of synapses as determined by ultrastructural measurements of type-XIV neurons in goldfish tectum<sup>28</sup>. Furthermore, PSD-95:GFP was always excluded from the local axonal arborization, which arises from the proximal dendritic segment. All of these observations are consistent with PSD-95:GFP acting as a postsynaptic marker. See Methods and **Supplementary Figures 1 and 2** online for further validation. Tectal cells expressing PSD-95:GFP and DsRed showed similar growth to cells expressing only GFP, indicating that neither protein perturbed tectal cell development (see **Supplementary Fig. 3** online).

Imaging of individual tectal cells on consecutive days revealed that total arbor length and number of PSD-95:GFP puncta (hereafter referred to simply as PSD puncta) increased dramatically between 3 and

<sup>1</sup>Neurosciences Program and <sup>2</sup>Department of Molecular and Cellular Physiology, Beckman Center, Stanford University, Stanford, California 94305, USA. <sup>3</sup>These authors contributed equally to this work. Correspondence should be addressed to S.J.S. (sjsmith@stanford.edu).

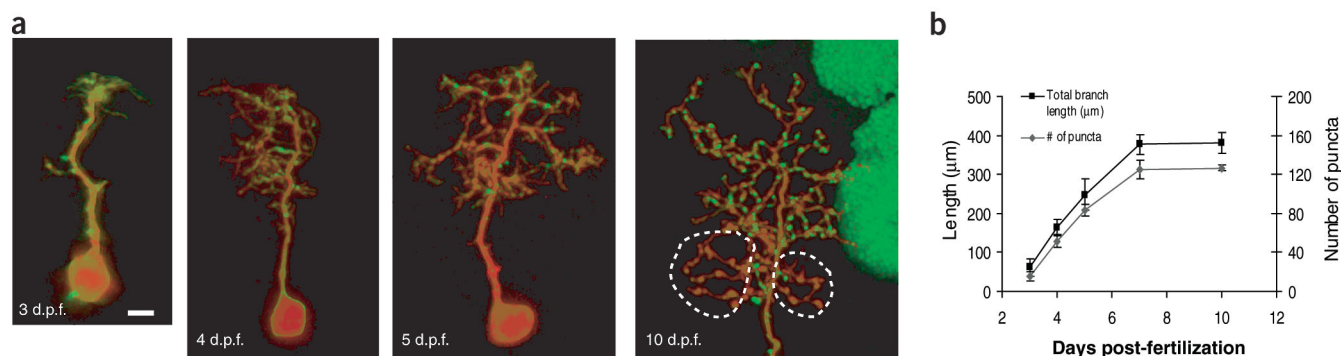


**Figure 1** Imaging of individual cells on consecutive days reveals that punctum formation and dendrite growth are concurrent processes. (a) Time series showing the same tectal cell imaged at 3, 4, 5 and 10 d.p.f.. PSD-95:GFP is excluded from the local axonal arborization (dotted line). Auto-fluorescence of the skin is visible in the upper-right corner of 10 d.p.f. Scale bar, 10 μm. (b) Quantification of total branch length and number of puncta. Data are expressed as means ( $\pm$  standard error, s.e.m.) from six cells.

7 d.p.f., after which time both the structure of the arbor and the number of puncta remained relatively stable (Fig. 1b). Increase in arbor length and punctum number occurred simultaneously, as demonstrated by the fact that punctum density on dendritic branches remained nearly constant (from  $0.28 \pm 0.05$  puncta/μm at 3 d.p.f. to  $0.35 \pm 0.02$  puncta/μm at 10 d.p.f.). Thus, arbor growth and PSD punctum formation in the zebrafish tectum are closely concurrent, with very little lag time between extension of a new dendritic process and formation of puncta upon it.

#### Only a small fraction of PSD puncta are stabilized

To examine the dynamics of synapse formation in relation to arbor growth, we performed time-lapse imaging of immature dendrites in the intact larval zebrafish at 20-min intervals for up to 24 h. A series of still

images from such a time-lapse session beginning at 3 d.p.f. shows significant growth of the arbor during this period, along with the formation of new PSD puncta (Fig. 2a and **Supplementary Video 2** online). Time-lapse imaging revealed an abundance of transient fine terminal processes rapidly extending and retracting, which gradually decreased over the course of development. Separate imaging experiments with an actin:GFP fusion show that all such dynamic protrusions are enriched in actin (**Supplementary Video 1** online). Because they satisfy the common morphological, dynamic and cytoskeletal criteria<sup>20,29–31</sup>, we henceforth refer to newly-formed motile protrusions as filopodia.

Time-lapse movies also show both stable PSD puncta and a large population of short-lived transient puncta (Fig. 2b and **Supplementary Video 3** online). Figure 2c shows the lifetimes of new puncta that were

observed from the time of their first appearance. The histogram reveals a population of PSD puncta with short lifetimes, as well as a wide distribution of puncta with longer lifetimes. We selected 3 h as a threshold between these two populations, which served to classify puncta into the categories of unstable or stable. As the arbor matures, the number of stable PSD puncta increases markedly, whereas the number of unstable puncta decreases (Fig. 2d).

When they first appear, puncta that become eliminated are indistinguishable from the initial appearance of puncta that persist and go on to form long-lasting stable

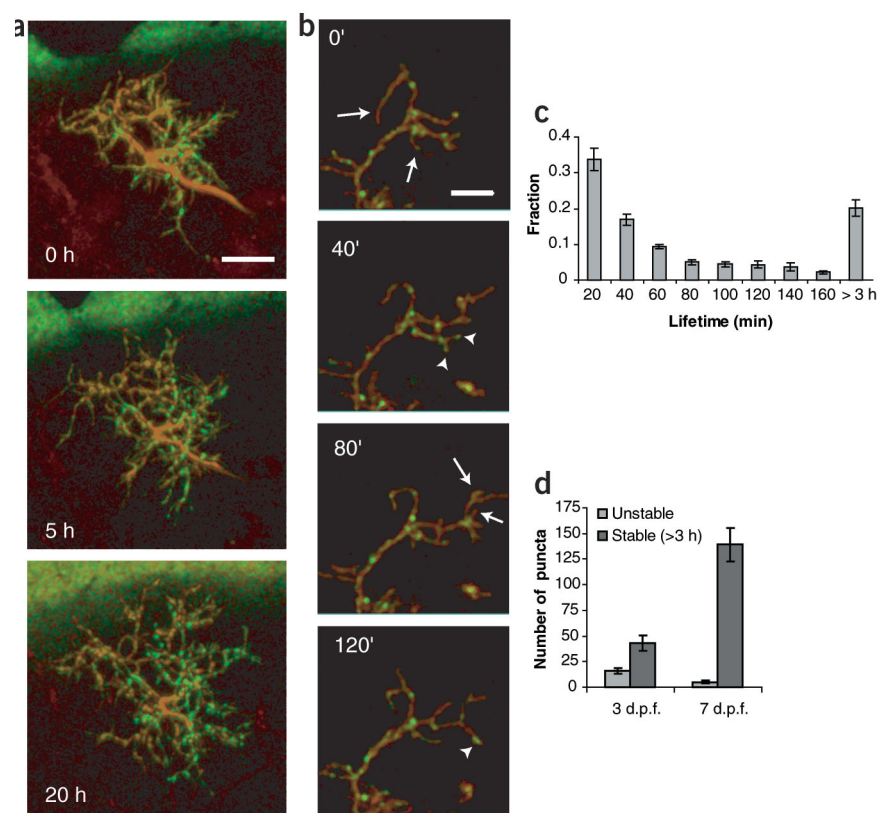


**Figure 2** Long-term imaging of arbor growth and punctum formation. (a) Series of still images from an extended time-lapse session started at 3 d.p.f. showing growth of the arbor and new puncta formation. Scale bar, 10 μm. (b) Series of images at 40-min intervals showing that arbor growth is characterized by the presence of many transient filopodia and puncta, indicated by arrows and arrowheads, respectively. Scale bar, 5 μm. (c) Analysis of new puncta lifetimes between 3 and 4 d.p.f. show that most persist for less than 3 h. (d) As dendritic arbors mature, the number of stable puncta increases, while the number of unstable puncta decreases. In c and d, data are expressed as mean  $\pm$  s.e.m. from six cells.

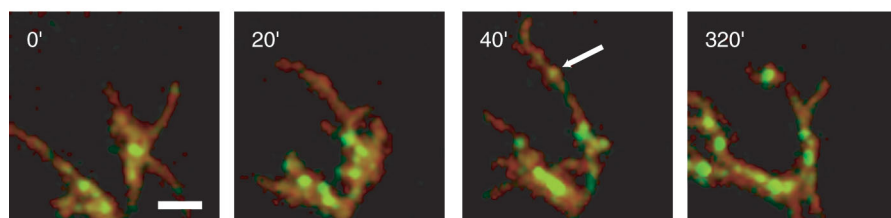


**Figure 3** Analysis of 'punctum-centric' movies reveals a typical mode of dendrite growth and puncta formation. A series of images from a time lapse showing a filopodium extending (20'), a punctum forming on it (40', indicated by arrow), which gradually increases in intensity, and the filopodium retracting back to the position of the stable punctum (320'). Scale bar, 3  $\mu$ m.

puncta, suggesting that these transient puncta may represent nascent synapses that undergo elimination<sup>32</sup>. This view is supported by previous *in vitro* studies, which have shown that even among populations of rapidly remodeling PSDs, almost all PSD-95:GFP puncta colocalize with presynaptic partners<sup>16</sup>. Similar instability of presynaptic assemblies has also been demonstrated, at longer imaging intervals, in *Xenopus laevis* optic tectum<sup>33</sup>.

These results show that the period of rapid dendritic arbor growth is characterized by the appearance of transient filopodia, as well as the formation of many PSD puncta, a subset of which are maintained leading to a gradual accumulation of stable puncta over time.

#### Dendritic filopodia are sites of PSD punctum formation

To allow systematic quantitative characterization of the dynamics of PSD punctum formation, we generated 'punctum-centric' movies of each individual punctum observed in time-lapse movies. We focused this analysis on the population of stable puncta, which persisted for more than 3 h. Previous studies of the time course of synapse assembly suggest that these represent functional synapses<sup>26,34</sup>. Consistent with previous observations, we found that new puncta appear *de novo* by gradual accretion, rather than stabilization of intact, preassembled puncta (transport packets), on a timescale similar to that observed *in vitro*<sup>26</sup>. The vast majority ( $94 \pm 2\%$ ;  $n = 6$  cells) of new stable puncta appear on filopodia, with only a small fraction forming on the stable shaft of the dendrite, either *de novo* ( $3 \pm 2\%$ ) or by apparent splitting of a previously existing punctum ( $3 \pm 2\%$ ). This splitting may simply be due to two unresolved neighboring puncta becoming visible due to small movements separating them by a distance greater than the resolution limit of the microscope.

Frames from a typical punctum-centric movie (Fig. 3 and Supplementary Video 4 online) illustrate the predominant mode of stable PSD punctum formation on a growing dendrite. A filopodium extends from the main branch, upon which a new punctum appears. The filopodium eventually retracts back to the position of the nascent punctum, which gradually grows in intensity and persists up to 5 h later on what becomes a stable branch of the dendrite. Although this example, for clarity, shows growth stopping after a

single punctum appears, often more than one punctum can appear on an extending filopodium. Furthermore, we often observed new filopodia sprouting from a recently stabilized branch, leading to further growth along this path. Both of these processes are illustrated in the sequence shown in Figure 4.

Electron microscopy and *in vitro* time-lapse studies of hippocampal neurons have led to the proposal that synapses on filopodia convert to shaft synapses by moving along a filopodium or being pulled into the shaft of the dendrite<sup>35,36</sup>. We have not observed such processes in our imaging

studies, rather, puncta on filopodia appear to become shaft puncta by conversion of the filopodium into a stable branch. Systematic characterization of 'branch-centric' movies, sub-volumes centered on branches, revealed that all net elaboration of the arbor, after initial pathfinding to the target area, is a result of iterated filopodial stabilization as shown in Figure 4. A branch can elongate by a succession of filopodia extending from its tip. Likewise, branching points form when two filopodia are stabilized from an endpoint, or when a filopodium extends from a midpoint on a branch segment. Thus, filopodia can serve as the site of PSD punctum formation, and filopodial stabilization leads to growth of the dendrite.

#### Filopodia are stabilized at sites of PSD puncta

Two different interpretations might be consistent with the correlations of branch and synapse stabilization evident from our data (Figs. 3 and 4). One is that formation of a synapse, as marked by a stable PSD punctum, plays an essential role in stabilizing the filopodium on which it is located. Alternatively, filopodia could be stabilized by a

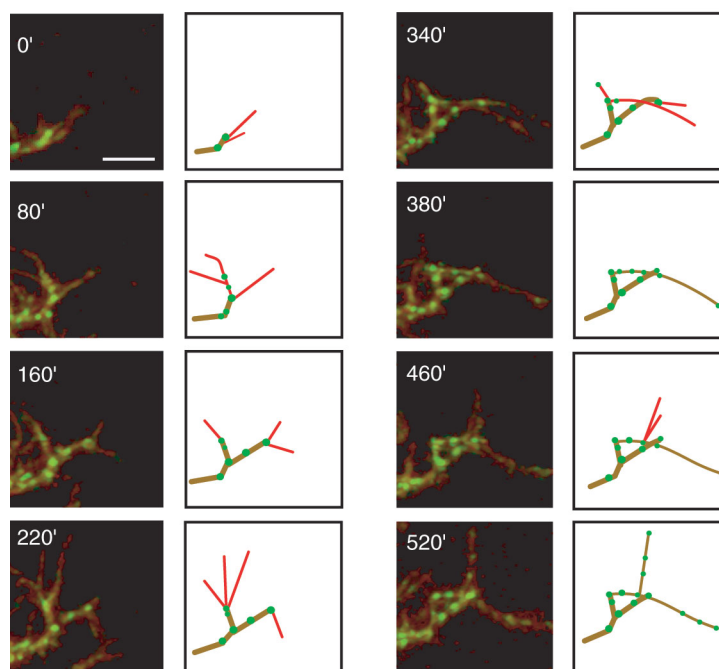


**Figure 4** Dendrite growth occurs by an iterative sequence of selective filopodial stabilization and punctum formation. Still images from a time-lapse series, accompanied by a schematic rendering for clarity. Green represents PSD-95:GFP puncta, red lines are newly formed (often transient) branches, and brown are persistent branches. Scale bar, 5  $\mu$ m.



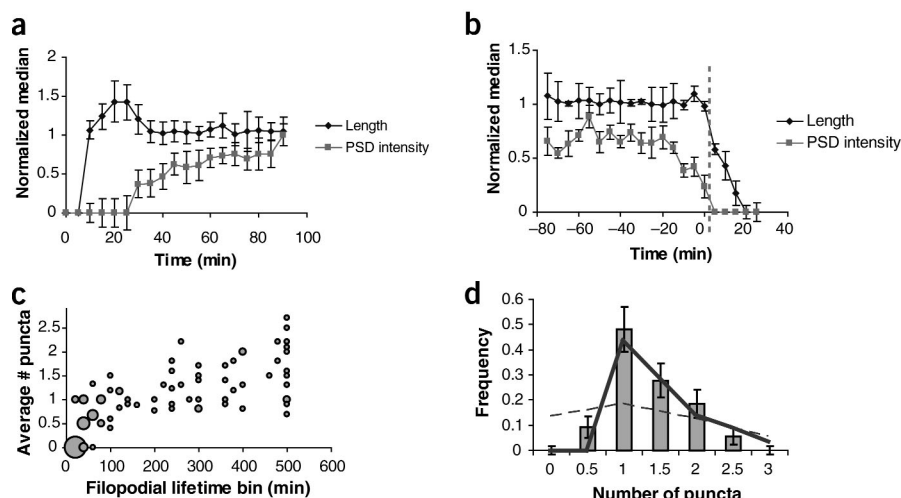


**Figure 5** PSD puncta and selective stabilization of dendritic filopodia. **(a)** Quantification of all observed single-punctum formation events (average of 15 events from four cells) reveals that filopodia retract back to the position of the stable punctum. Filopodial length in **a** and **b** is normalized to the position of punctum formation and median-averaged. **(b)** Quantification of all observed retracted filopodia bearing a single punctum at 5-min intervals demonstrates that retraction is preceded by punctum disassembly (average of 9 retraction events from four cells). **(c)** Number of puncta on terminal dendritic processes versus lifetime of that process. Terminal processes do not persist without bearing at least one punctum ( $n = 5$  cells). Area of a point corresponds to number of overlapping data points. **(d)** Histogram of number of puncta on all terminal dendritic processes persisting for longer than 1 h shows a marked absence of processes with zero puncta. Dashed curve shows a Poisson distribution, solid curve shows the prediction for Poisson distribution followed by elimination. Lifetime is binned by number of 20-min interval time points it was observed in. That is, a filopodium labeled as 60 min could have persisted from 41 min to 79 min, due to sampling interval.

synapse-independent mechanism, which then incidentally permits the eventual formation of a synapse upon that stable structure. Three lines of evidence support the first interpretation. First, we performed a quantification of all filopodia observed at high temporal resolution (5-min intervals) which formed a single punctum. Retrospectively normalizing filopodial length to the position where the nascent punctum formed reveals that the process illustrated in **Figure 3** is in fact typical. Filopodia most commonly overextend, then retract back to the location of a newly formed punctum, which appears approximately 30 minutes after filopodial extension and gradually increases in intensity (**Fig. 5a**). The fact that the filopodium does not stabilize at an arbitrary length suggests that the point of punctum formation plays a crucial role in the stabilization process.

Secondly, filopodia bearing puncta are not always stable indefinitely, and quantitative analysis of such cases where filopodia bearing PSD puncta are eliminated reveals that the start of filopodial retraction is preceded by disassembly of the anchoring PSD punctum. **Figure 5b** shows a compilation of the time course of all retraction events observed at high temporal resolution involving filopodia bearing a single punctum. Beginning up to 20 min before the start of filopodial retraction, the punctum undergoes a progressive and significant decrease in intensity, suggesting that prior elimination of the nascent synapse destabilizes the filopodium. Such a process has been demonstrated for presynaptic terminals at the neuromuscular junction<sup>37</sup>.

Finally, if synapses as marked by PSD puncta are indeed necessary for the stabiliza-

tion of a dendritic branch, one would expect every stable branch to bear at least one PSD punctum. Conversely, if branch stabilization is not dependent on the presence of a PSD punctum, one might expect some stable processes that, by chance, do not bear any puncta. **Figure 5c** shows the number of puncta on all terminal filopodia and branches versus the lifetime of that dendritic process, measured from 'branch-centric' movies. Although short-lived filopodia often do not bear PSD puncta, no terminal processes persist longer than one hour without bearing a punctum. Averages over the lifetime of a branch can be less than one, because PSD puncta often take up to 30 min to appear, and can disassemble prior to retraction (**Fig. 5a,b**).

This is further characterized in a histogram of the number of puncta appearing on all processes lasting longer than one hour (**Fig. 5d**). If appearance of a punctum were a random event, one would expect some cases where a stabilized filopodium happens not to bear a punctum. In particular, if punctum formation did not influence branch stabilization and followed Poisson statistics, for the given mean (1.36 puncta per process), one would expect nearly the same number of filopodia with zero puncta as with one punctum (dashed curve). On the other hand, a

model where puncta form by a Poisson process with a mean less than one, followed by elimination of all filopodia without at least one punctum, is much closer to the data (solid curve). Thus, all dendritic processes that persist have at least one punctum for the majority of their lifetime, and the distribution suggests that filopodia or branches that do not bear PSD puncta are invariably eliminated.

These three lines of evidence together demonstrate that the site marked by a PSD-95:GFP punctum has a crucial role in the stabilization of a small subset from the pool of mostly transient filopodia. Because PSD-95:GFP likely marks postsynaptic assembly, this suggests that the presence of a nascent synapse could selectively stabilize filopodia, which become dendritic branches from which iterative rounds of such growth can occur.

## DISCUSSION

Our long-term *in vivo* imaging has addressed several outstanding questions about the process of synapse formation on developing den-

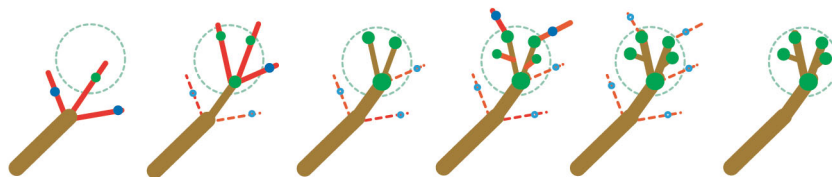


**Figure 6** Model of synaptotropic guidance of dendrite growth. A number of filopodia (solid red) extend from a dendritic branch. Those that encounter correct partners and form synaptic contacts (green dots) are stabilized as new branches (brown), whereas those that establish inappropriate contacts (blue dots) are retracted (dashed red). Successive rounds of selective stabilization result in arborization within a field of appropriate synaptic connections (dashed green region).

drites. First, the vast majority of PSD puncta form on dendritic filopodia, confirming earlier suggestions of a role in probing the environment for synaptic contacts<sup>19,35,36,38</sup>. However, previous studies could not address the transition between the presence of synapses on filopodia early in development and their eventual position on dendritic shafts or spines, leading to the proposition that synapses were either reeled in or could slide along filopodia. Our findings resolve this issue by showing that a small fraction of filopodia persist as stable branches, and that this is in fact the fundamental mechanism of growth in tectal cell dendrites. Thus, rather than needing to pull in an axon through dense neuropil, the dendrite essentially grows out to meet it via filopodial stabilization at the point of contact. Furthermore, this dual role of filopodia in both synaptogenesis and dendrite growth has significant implications for previous studies of molecular and physiological factors that can modulate filopodial dynamics<sup>29,39,40</sup>.

We present three lines of evidence suggesting that the formation of a stable synapse, indicated by a PSD punctum, can selectively stabilize filopodia, which eventually form branches from which further growth can occur. Figure 6 is an illustration of our model of how this process could result in directed growth. The fact that new growth occurs from previously stabilized filopodia creates a positive feedback, which can lead to increased exploration into target regions. Similarly, in regions devoid of synaptic partners, filopodia would not stabilize, and arborization in these regions would be inhibited. This provides a mechanism for self-organization of synaptic connections that would shape circuit topography. Remarkably, this process of synapse formation and dendrite guidance was proposed over a decade ago<sup>41,42</sup> as a "synaptotropic hypothesis" of dendrite growth, based solely on studies of fixed tissue. However, this live *in vivo* imaging provides the first direct observation of this mode of dendrite growth and branching.

The fate of a filopodium, and thus the growth and branching of the arbor, would depend on the formation and subsequent stabilization or disassembly of a nascent synapse. Synapse stability could be based on many factors, such as complementary adhesion molecules, intercellular signaling between pre- and postsynaptic neurons, or synaptic transmission and coincident activity<sup>43</sup>. This would imply that the effects of sensory activity on arbor elaboration<sup>7</sup> could in fact be mediated by effects on synapse stabilization<sup>44</sup>.

Likewise, it is not clear what aspects of nascent synapse formation result in stabilization of a filopodium. The structural underpinnings of the synapse, both adhesion across the synaptic cleft and cytoskeletal anchoring within the dendrite, could provide mechanical support. N-cadherin, an adhesion molecule that localizes to sites of synaptic contact, is part of a Wnt/ $\beta$ -catenin pathway which has been shown to mediate dendritic growth<sup>45</sup>. It has also been shown that intracellular calcium release evoked by neurotransmitters can maintain dendritic processes<sup>9</sup>, suggesting that synaptic transmission at the nascent synapse could play a stabilizing role not only for the synapse itself but for the form of the arbor.

The degree to which a synaptotropic mode of growth shapes dendritic arbors of other cell types remains to be explored. For example, in relatively un-branched spiny dendrites, filopodia which establish synaptic contact may be stabilized as spines, rather than new branches. However, in general this process can provide a mechanism for directing growth into regions of appropriate synaptic contacts, and implies that the factors that determine synapse stabilization discussed above are brought to bear in shaping the dendrite itself. The synaptotropic mode of growth would ensure the matching of dendritic morphology with a specific set of synaptic connections, and hence may be a key element in the appropriate development of functional neural circuitry.

## METHODS

**Generation of PSD-95:GFP plasmid.** Searches of GenBank databases identified a zebrafish EST clone encoding a protein with high sequence homology to the guanylate kinase domain of mammalian MAGUK family proteins, of which PSD-95 is a member. This EST sequence was used to probe an adult zebrafish retina cDNA library. Iterative rounds of screening using progressively more 5' probes resulted in the isolation of a single clone encoding full-length zebrafish PSD-95. Zebrafish PSD-95 was PCR amplified using the primer pairs: 5'-GGAATTCGTCGCCACCATGCCTCTCAAACGAGAAGATAC-3' and 3'-GACCTAGGGTCGTCGTCTCTCTGACCTCCTCTGGGCCC-5', which generated an *Eco*R1 site, a Kozak consensus sequence immediately 5' to the translational start codon of PSD-95, a tri-glycine linker, and a *Sma*I site at the extreme 3' terminus of PSD-95. The PCR-amplified PSD-95 was fused in-frame to EGFP (Clontech). An upstream activator sequence (UAS)<sup>46</sup> was cloned into the multiple cloning site immediately upstream of PSD-95 to generate UAS:PSD-95:GFP. UAS was also cloned into the multiple cloning site of *pDsRed-Express-1* (Clontech) to generate UAS:DsRed-Express. The UAS:PSD-95:GFP fragment was subcloned into the UAS:DsRed-Express-1 plasmid to generate UAS:PSD-95:GFP:UAS:DsRed-Express.

**Validation of PSD-95:GFP as a synaptic marker.** Although the localization of PSD-95:GFP is consistent with it acting as a postsynaptic marker, we wanted to validate this further by examining the degree of colocalization of PSD-95:GFP with a known presynaptic marker. Fish expressing PSD-95:GFP in tectal cells were fixed and wholemount labeled as described<sup>47</sup> with an antibody to SV2. Presumably as a result of high synapse density in the tectal neuropil, SV2 staining was extremely dense, making it impossible to show meaningful colocalization of SV2 puncta with PSD-95:GFP puncta (see **Supplementary Fig. 1** online). However, in dissociated immature rat hippocampal cultures, where synapse density is much lower, we were able to show that our zebrafish PSD-95:GFP had a punctate distribution in dendrites and that 86% of GFP puncta colocalized with immunolabeled synaptophysin puncta (see **Supplementary Fig. 2** online). Culturing and transfection were performed as described<sup>48</sup>. For immunolabeling, hippocampal cells were fixed in 4% paraformaldehyde, 4% sucrose for 20 min at room temperature, and labeling was performed as described<sup>49</sup>. Comparison of dendritic branch length over multiple days of development, between cells expressing PSD-95:GFP + DsRed, versus GFP-labeled control cells (see **Supplementary Fig. 3** online), showed no significant difference, indicating that expression of PSD95:GFP and DsRed did not perturb tectal cell development. Also, in tectal cells there was no systematic variation in the density or intensity of PSD-95:GFP puncta with distance from the soma, indicating that the GFP puncta we observed are not nonspecific aggregations resulting from overexpression. Furthermore, PSD-95 is known to form head-to-head multimers<sup>50</sup>, making it likely that PSD-95:GFP is binding to, and recapitulating the expression of, endogenous PSD-95.

**DNA preparation and microinjection of zebrafish embryos.** Raising, maintaining and spawning of adult zebrafish were performed as described<sup>47</sup>. All procedures were approved by the Institutional Animal Care and Use Committee of Stanford University. The pan-neuronal goldfish *alpha-1 tubulin* promoter was used to drive *Gal4-VPI6* expression on an activator plasmid<sup>46</sup>. This was used in conjunction with the PSD-95:GFP effector plasmid to drive mosaic transient expression in zebrafish embryos. Plasmid DNA was prepared using Qiagen miniprep kits, and both effector and activator plasmids were injected at a concentration of 25 ng/ $\mu$ l in 0.1M KCl into 1–4 cell stage zebrafish embryos. Injected embryos were raised at 28 °C, in fish water containing methylene blue and phenylthiourea to block pigment formation.

**Imaging.** Zebrafish larvae from 3–10 d.p.f. were mounted on a microscope slide imaging chamber in 1% agarose and covered with embryo medium<sup>47</sup>. The agarose was sufficient to restrain movements of the larvae so that anesthesia was not required. Larvae could be maintained in this configuration for imaging sessions up to 24 h, at the end of which they appeared healthy and continued to develop normally. Imaging was performed on a custom-built two-photon microscope with a 63 $\times$ /0.9NA water-immersion objective (Zeiss). Excitation was provided by a Mira 900 Ti:Sapphire femtosecond pulsed laser system (Coherent) tuned to 920 nm, which allowed efficient simultaneous

excitation of GFP and DsRed-Express. Up to forty optical sections were obtained at 1–1.5  $\mu\text{m}$  intervals for each time point, using custom acquisition software (N. Ziv, Rappaport Institute, Israel). Except for punctum-centric movies, all analyses used the full 3D dataset.

**Image analysis.** Image processing and analysis was performed with custom Matlab software (Mathworks). Two-color sections were median filtered to reduce dark noise and shot noise, and subjected to a ratio-preserving gamma correction, which enhanced visibility of fine structures such as filopodia without distorting the use of the DsRed-Express channel to normalize PSD-95:GFP levels to cytosolic volume. Branch length was measured by tracing the dendritic arbor through three dimensions. The local axonal arbor was identified by its stereotyped U-turn initiation in layer 4/5, the presence of varicosities, and the exclusion of PSD-95:GFP, and was not included in dendritic arbor length.

Individual puncta were identified in single sections as localized increases in the ratio of PSD-95:GFP to DsRed-Express which were greater than two pixels (0.35  $\mu\text{m}$ ) in diameter. Custom software was used to track the 3D coordinates of each punctum through consecutive frames of a time-lapse video. These coordinates were then used to create punctum-centric movies, which were maximum-intensity projections of a small subvolume centered on the location of each identified punctum. These movies allowed every punctum observed to be scored for characteristics such as site or mode of appearance.

Extension and retraction events were measured from high temporal resolution (5 min) movies spanning approximately 5 h. This shorter total imaging time restricted the number of extension and retraction events that could be observed unobscured in their entirety; all such events were analyzed and compiled in Figure 5a,b. Punctum intensity was measured by totaling the corrected PSD-95:GFP fluorescence for each pixel within a rectangle surrounding the punctum. Corrected PSD-95:GFP fluorescence was calculated by multiplying the DsRed value in a pixel by the ratio of GFP to DsRed-Express in a neighboring non-punctate region of the branch, and subtracting this value from the PSD-95:GFP intensity. This allowed correction both for small bleed-through of DsRed emission into the GFP channel, and the relatively uniform level of non-punctate GFP.

Lifetimes of terminal dendritic processes (Fig. 5c,d) were measured by marking all such processes at one time point within a time lapse, and generating sub-volume movies centered on them. These movies were scored for total lifetime, as well as number of puncta in each frame, which was used to generate the average number of puncta on the process over its lifetime. Theoretical curves were: dashed, Poisson distribution  $P(N, n_{\text{obs}})$  with the observed mean  $n_{\text{obs}}$ , and solid, modified Poisson distribution to include hypothesized effect of elimination of filopodia, defined by  $P_{\text{stab}}(N < 1) = 0$  and  $P_{\text{stab}}(N \geq 1) = P(N, n_{\text{pre}})$ , where  $n_{\text{pre}}$  was calculated such that the mean of  $P_{\text{stab}}$  equals  $n_{\text{obs}}$ .

GenBank accession number for PSD-95: AY520570.

Note: Supplementary information is available on the Nature Neuroscience website.

## ACKNOWLEDGMENTS

We thank B. Barres, L. Luo, W. Talbot and R. Tsien for their comments on the manuscript. GAL4-VP16/UAS expression constructs were graciously provided by S. Fraser. This work was supported by the Wellcome Trust (M.P.M.), Howard Hughes Medical Institute (C.M.N.), the Vincent and Stella Coates Foundation and the National Institute of Neurological Disorders and Stroke (NS043461).

## COMPETING INTERESTS STATEMENT

The authors declare that they have no competing financial interests.

Received 4 November 2003; accepted 14 January 2004

Published online at <http://www.nature.com/natureneuroscience/>

- Kaethner, R.J. & Stuermer, C.A. Dynamics of process formation during differentiation of tectal neurons in embryonic zebrafish. *J. Neurobiol.* **32**, 627–639 (1997).
- Jontes, J.D., Buchanan, J. & Smith, S.J. Growth cone and dendrite dynamics in zebrafish embryos: early events in synaptogenesis imaged *in vivo*. *Nat. Neurosci.* **3**, 231–237 (2000).
- Wu, G.Y., Zou, D.J., Rajan, I. & Cline, H. Dendritic dynamics *in vivo* change during neuronal maturation. *J. Neurosci.* **19**, 4472–4483 (1999).

- Grueber, W.B., Jan, L.Y. & Jan, Y.N. Different levels of the homeodomain protein cut regulate distinct dendrite branching patterns of *Drosophila* multidendritic neurons. *Cell* **112**, 805–818 (2003).
- Komiyama, T., Johnson, W.A., Luo, L. & Jefferis, G.S. From lineage to wiring specificity. POU domain transcription factors control precise connections of *Drosophila* olfactory projection neurons. *Cell* **112**, 157–167 (2003).
- Furrer, M.P., Kim, S., Wolf, B. & Chiba, A. Robo and Frazzled/DCC mediate dendritic guidance at the CNS midline. *Nat. Neurosci.* **6**, 223–230 (2003).
- Sin, W.C., Haas, K., Ruthazer, E.S. & Cline, H.T. Dendrite growth increased by visual activity requires NMDA receptor and Rho GTPases. *Nature* **419**, 475–480 (2002).
- Horch, H.W. & Katz, L.C. BDNF release from single cells elicits local dendritic growth in nearby neurons. *Nat. Neurosci.* **5**, 1177–1184 (2002).
- Lohmann, C., Myhr, K.L. & Wong, R.O. Transmitter-evoked local calcium release stabilizes developing dendrites. *Nature* **418**, 177–181 (2002).
- Cline, H.T. Dendritic arbor development and synaptogenesis. *Curr. Opin. Neurobiol.* **11**, 118–126 (2001).
- Scott, E.K. & Luo, L. How do dendrites take their shape? *Nat. Neurosci.* **4**, 359–365 (2001).
- Jan, Y.N. & Jan, L.Y. Dendrites. *Genes Dev.* **15**, 2627–2641 (2001).
- Wong, R.O. & Ghosh, A. Activity-dependent regulation of dendritic growth and patterning. *Nat. Rev. Neurosci.* **3**, 803–812 (2002).
- Garner, C.C., Zhai, R.G., Gundelfinger, E.D. & Ziv, N.E. Molecular mechanisms of CNS synaptogenesis. *Trends Neurosci.* **25**, 243–251 (2002).
- McGee, A.W. & Brecht, D.S. Assembly and plasticity of the glutamatergic postsynaptic specialization. *Curr. Opin. Neurobiol.* **13**, 111–118 (2003).
- Marrs, G.S., Green, S.H. & Dailey, M.E. Rapid formation and remodeling of postsynaptic densities in developing dendrites. *Nat. Neurosci.* **4**, 1006–1013 (2001).
- Cohen-Cory, S. The developing synapse: construction and modulation of synaptic structures and circuits. *Science* **298**, 770–776 (2002).
- Washbourne, P., Bennett, J.E. & McAllister, A.K. Rapid recruitment of NMDA receptor transport packets to nascent synapses. *Nat. Neurosci.* **5**, 751–759 (2002).
- Wong, W.T. & Wong, R.O. Rapid dendritic movements during synapse formation and rearrangement. *Curr. Opin. Neurobiol.* **10**, 118–124 (2000).
- Portera-Cailliau, C., Pan, D.T. & Yuste, R. Activity-regulated dynamic behavior of early dendritic protrusions: evidence for different types of dendritic filopodia. *J. Neurosci.* **23**, 7129–7142 (2003).
- Sheng, M. Molecular organization of the postsynaptic specialization. *Proc. Natl. Acad. Sci. USA* **98**, 7058–7061 (2001).
- Prange, O. & Murphy, T.H. Modular transport of postsynaptic density-95 clusters and association with stable spine precursors during early development of cortical neurons. *J. Neurosci.* **21**, 9325–9333 (2001).
- Rao, A., Kim, E., Sheng, M. & Craig, A.M. Heterogeneity in the molecular composition of excitatory postsynaptic sites during development of hippocampal neurons in culture. *J. Neurosci.* **18**, 1217–1229 (1998).
- Ebihara, T., Kawabata, I., Usui, S., Sobue, K. & Okabe, S. Synchronized formation and remodeling of postsynaptic densities: long-term visualization of hippocampal neurons expressing postsynaptic density proteins tagged with green fluorescent protein. *J. Neurosci.* **23**, 2170–2181 (2003).
- Gleason, M.R. *et al.* Translocation of CaM kinase II to synaptic sites *in vivo*. *Nat. Neurosci.* **6**, 217–218 (2003).
- Bresler, T. *et al.* The dynamics of SAP90/PSD-95 recruitment to new synaptic junctions. *Mol. Cell Neurosci.* **18**, 149–167 (2001).
- Douglas, R.H. & Djamgoz, M.B.A. (eds.). *The Visual System of Fish* (Chapman and Hall, Ltd., London, 1990).
- Meek, J. A Golgi-electron microscopic study of goldfish optic tectum. II. Quantitative aspects of synaptic organization. *J. Comp. Neurol.* **199**, 175–190 (1981).
- Lendvai, B., Stern, E.A., Chen, B. & Svoboda, K. Experience-dependent plasticity of dendritic spines in the developing rat barrel cortex *in vivo*. *Nature* **404**, 876–881 (2000).
- Grutzendler, J., Kasthuri, N. & Gan, W.B. Long-term dendritic spine stability in the adult cortex. *Nature* **420**, 812–816 (2002).
- Matus, A. Actin-based plasticity in dendritic spines. *Science* **290**, 754–758 (2000).
- Lichtman, J.W. & Colman, H. Synapse elimination and indelible memory. *Neuron* **25**, 269–278 (2000).
- Alsina, B., Vu, T. & Cohen-Cory, S. Visualizing synapse formation in arborizing optic axons *in vivo*: dynamics and modulation by BDNF. *Nat. Neurosci.* **4**, 1093–1101 (2001).
- Friedman, H.V., Bresler, T., Garner, C.C. & Ziv, N.E. Assembly of new individual excitatory synapses: time course and temporal order of synaptic molecule recruitment. *Neuron* **27**, 57–69 (2000).
- Fiala, J.C., Feinberg, M., Popov, V. & Harris, K.M. Synaptogenesis via dendritic filopodia in developing hippocampal area CA1. *J. Neurosci.* **18**, 8900–8911 (1998).
- Ziv, N.E. & Smith, S.J. Evidence for a role of dendritic filopodia in synaptogenesis and spine formation. *Neuron* **17**, 91–102 (1996).
- Colman, H., Nabekura, J. & Lichtman, J.W. Alterations in synaptic strength preceding axon withdrawal. *Science* **275**, 356–361 (1997).
- Dunaevsky, A. & Mason, C.A. Spine motility: a means towards an end? *Trends Neurosci.* **26**, 155–160 (2003).
- Tashiro, A., Dunaevsky, A., Blazeski, R., Mason, C.A. & Yuste, R. Bidirectional regu-



- lation of hippocampal mossy fiber filopodial motility by kainate receptors. A two-step model of synaptogenesis. *Neuron* **38**, 773–784 (2003).
40. Wong, W.T. & Wong, R.O. Changing specificity of neurotransmitter regulation of rapid dendritic remodeling during synaptogenesis. *Nat. Neurosci.* **4**, 351–352 (2001).
  41. Vaughn, J.E., Barber, R.P. & Sims, T.J. Dendritic development and preferential growth into synaptogenic fields: a quantitative study of Golgi-impregnated spinal motor neurons. *Synapse* **2**, 69–78 (1988).
  42. Vaughn, J.E. Fine structure of synaptogenesis in the vertebrate central nervous system. *Synapse* **3**, 255–285 (1989).
  43. Ackermann, M. & Matus, A. Activity-induced targeting of profilin and stabilization of dendritic spine morphology. *Nat. Neurosci.* **6**, 1194–1200 (2003).
  44. Yoshii, A., Sheng, M.H. & Constantine-Paton, M. Eye opening induces a rapid dendritic localization of PSD-95 in central visual neurons. *Proc. Natl. Acad. Sci. USA* **100**, 1334–1339 (2003).
  45. Yu, X. & Malenka, R.C. beta-catenin is critical for dendritic morphogenesis. *Nat. Neurosci.* **6**, 1169–1177 (2003).
  46. Koster, R.W. & Fraser, S.E. Tracing transgene expression in living zebrafish embryos. *Dev. Biol.* **233**, 329–346 (2001).
  47. Westerfield, M. *The Zebrafish Book* (Institute of Neuroscience, University of Oregon, Eugene, 1993).
  48. Banker, G. & Goslin, K. (eds.) *Culturing Nerve Cells* (MIT Press, Cambridge, 1998).
  49. Micheva, K.D., Holz, R.W. & Smith, S.J. Regulation of presynaptic phosphatidylinositol 4,5-bisphosphate by neuronal activity. *J. Cell Biol.* **154**, 355–368 (2001).
  50. Hsueh, Y.P., Kim, E. & Sheng, M. Disulfide-linked head-to-head multimerization in the mechanism of ion channel clustering by PSD-95. *Neuron* **18**, 803–814 (1997).